

Geophysical Research Letters

Supporting Information for

Jupiter's Whistler-mode Belts and Electron Slot Region

Y.-X. Hao^{1,2}, Y. Y. Shprits^{1,3,4}, J. D. Menietti⁵, Z. Y. Liu⁶, T. Averkamp⁵, D. D. Wang¹,
P. Kollmann⁷, G. B. Hospodarsky⁵, A. Drozdov⁴, E. Roussos², N. Krupp², R. B. Horne⁸,
E. E. Woodfield⁸ and S. J. Bolton⁹

1. GFZ German Research Centre for Geosciences, 14473, Potsdam, Germany

2. Max Planck Institute for Solar System Research, 37077, Goettingen, Germany

3. Institute of Physics and Astrophysics, University of Potsdam, Germany

4. University of California Los Angeles, Los Angeles, CA, USA

5. Department of Physics and Astronomy, University of Iowa, Iowa City, USA

6. IRAP, CNRS-Universite Toulouse III Paul Sabatier, Toulouse, France

7. Johns Hopkins University Applied Physics Laboratory, Laurel, MD, USA

8. British Antarctic Survey, High Cross, Madingley Road, Cambridge, UK

9. Space Science and Engineering Division, Southwest Research Institute, San Antonio, TX, USA

Contents of this file

Figures S1 to S4

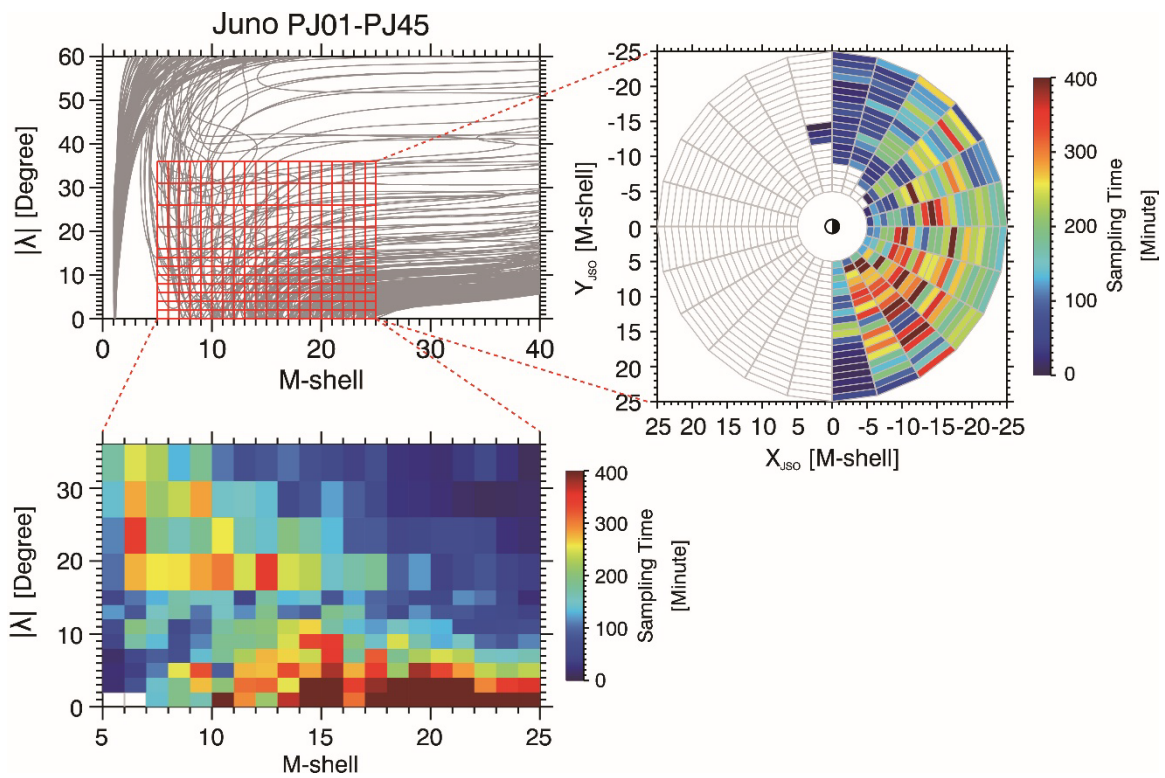


Figure S1. The orbit and sampling time of Juno spacecraft in magnetic coordinate system. Top left panel shows the PJ01-45 trajectories in $(M, |\lambda|)$ plane. Red lines depict the grid used in this study. Bottom panel shows the accumulative sampling time of Juno in each grid in $(M, |\lambda|)$ plane while the top right panel shows the (M, MLT) plane.

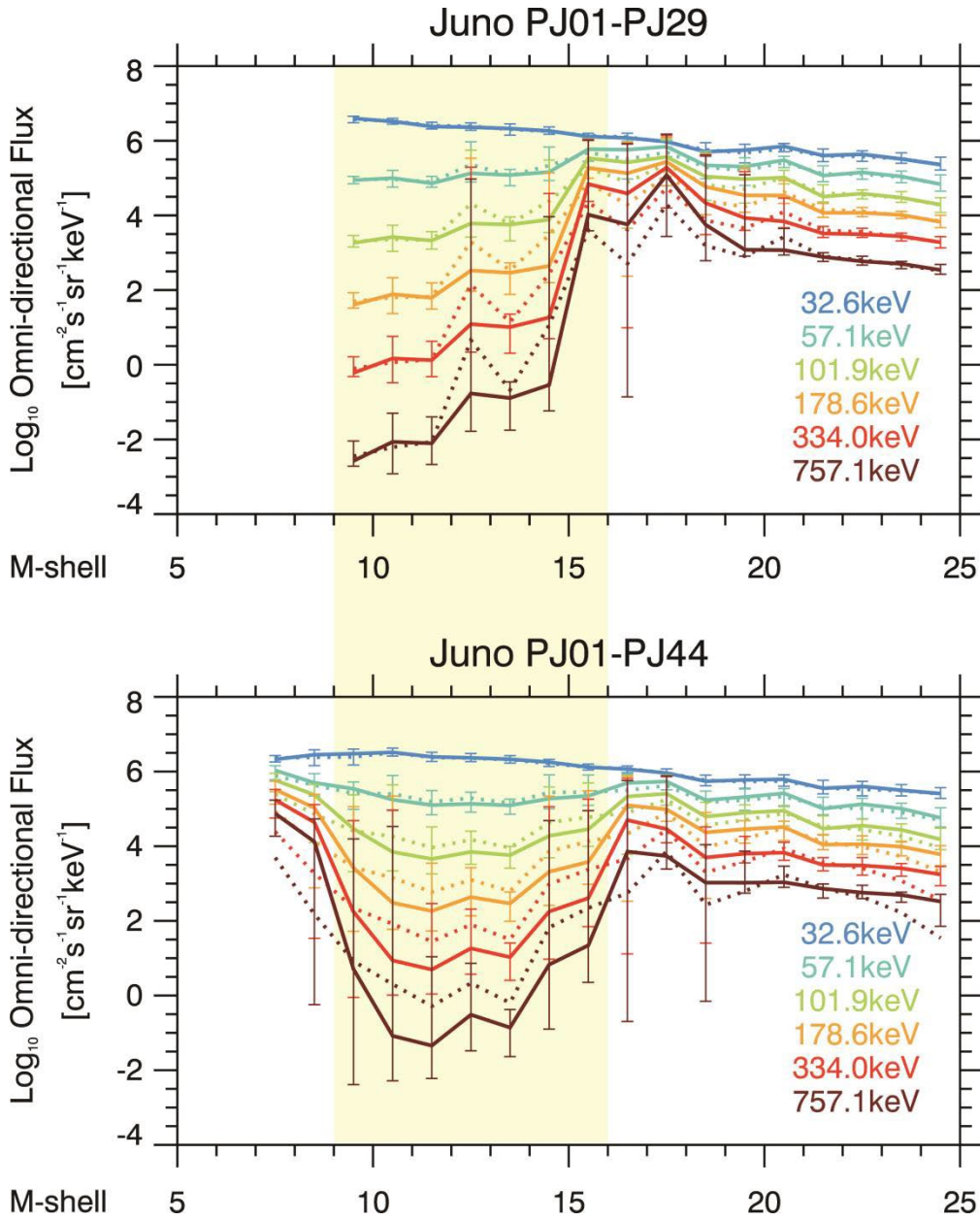


Figure S2. Near-equatorial differential electron fluxes as a function of M-shell measured by Juno/JEDI. Top panel shows the statistical results for the first 29 perijove orbits (corresponding to Ma et al. [2021]). Bottom Panel shows the results for the first 44 perijove orbits (same as Figure 3(b)). The solid curves show the median value of differential fluxes. Error bars denotes the upper and lower quartile. Dashed curves show the mean value.

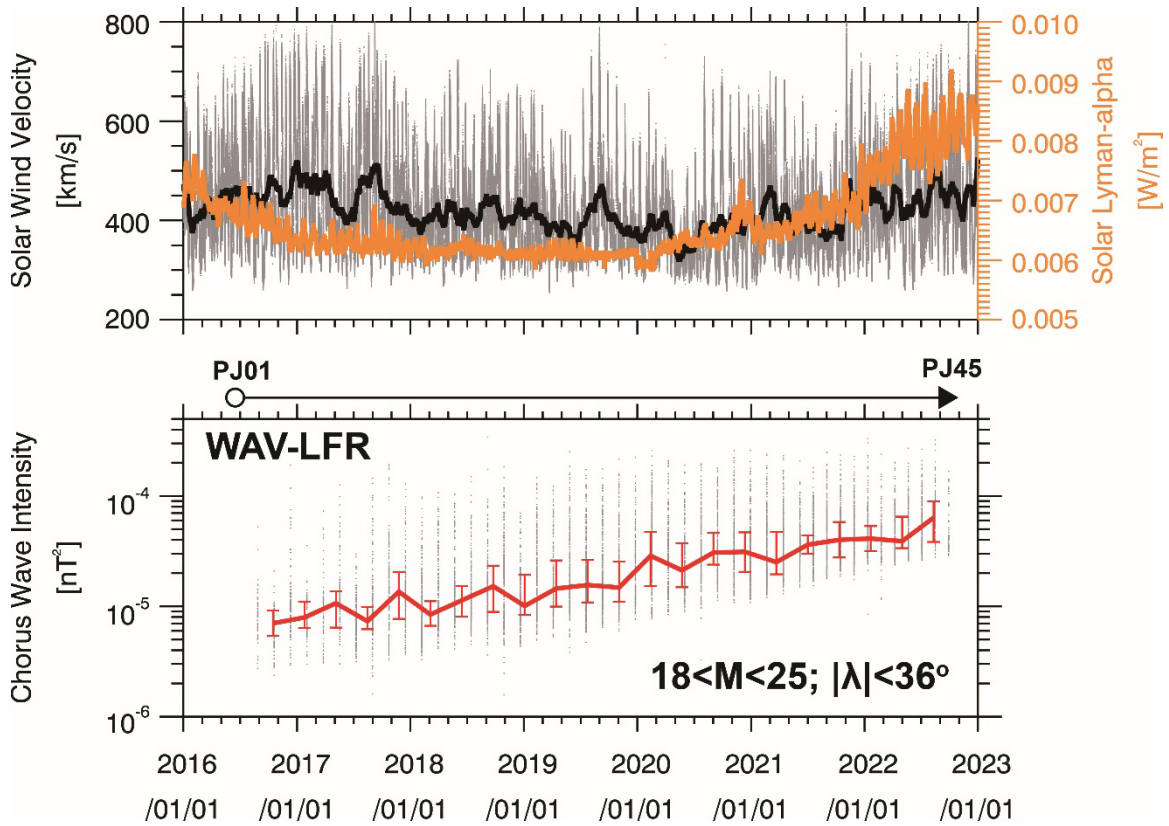


Figure S3. Top panel: solar activities during the time interval of this study. Grey dots show the 1-hour averaged solar wind velocity at 1 au. Black curve shows its 27-day running average. Orange curve show the solar Lyman-alpha radiation intensity. Bottom panel: time series of the outer belt chorus intensity. Grey dots show the 1-min $\langle B_w^2 \rangle$ data points of frequency-spectral integrated chorus intensity detected within $18 < M < 25$ and $|\lambda| < 36^\circ$. Red curve gives the median value. Error bars depict the upper and lower quartile.

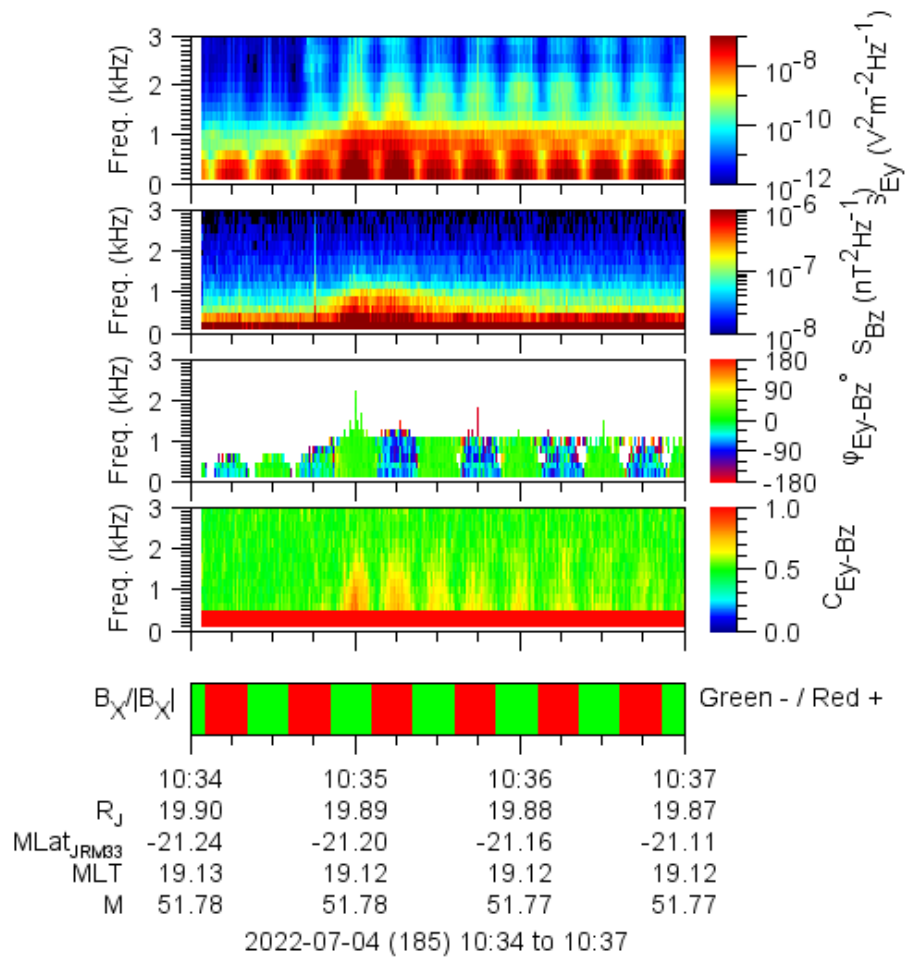


Figure S4. Waveform analysis for periods of burst mode (high resolution) Juno Waves instrument data. The data were obtained during a period of probable auroral hiss emission at large M-shell ($M > 20$). From top to bottom the panels are: E_y spectral density, B_z spectral density, mutual phase difference of $\phi_{E_y-B_z}$ (degrees), mutual coherence $C_{E_y-B_z}$, and the sign of the ambient magnetic field component in the spacecraft + x axis. Using the method and assumptions presented in Kolmasova et al. (2018), a comparison of the phase difference of the emissions in the third panel to the sign of ambient magnetic field along the spacecraft +x axis as the spacecraft rotates shows that the waves are propagating toward the magnetic equator, consistent with auroral hiss.